

**STRUCTURE AND PHASE TRANSITIONS  
OF AZOMETHINE BILIGAND COMPLEXES OF IRON(III)  
BASED ON 3,4,5-TRI(TETRADECYLOXY)BENZOYLOXY-  
4-SALICYLIDENE-N'-ETHYL-N-ETHYLENEDIAMINE**

**U. V. Chervonova<sup>1</sup>, M. S. Gruzdev<sup>1</sup>,  
A. M. Kolker<sup>1</sup>, and O. B. Akopova<sup>2</sup>**

UDC 54.057:544.17:544.015.4:544.16

New biligand complexes of iron(III) are synthesized based on 3,4,5-tri(tetradecyloxy)benzoyloxy-4-salicylidene-N'-ethyl-N-ethylenediamine azomethine with the outer sphere  $\text{NO}_3^-$ ,  $\text{PF}_6^-$ ,  $\text{Cl}^-$ ,  $\text{BF}_4^-$ ,  $\text{ClO}_4^-$ , and  $\text{CNS}^-$  anions. All the target compounds are characterized by gel exclusion chromatography, elemental analysis, and electron, IR, and NMR spectroscopy. The presence of complex-forming ions is confirmed by FT-IR spectra in the far region. The formation of biligand polychelate complexes with an octahedral packing of the iron ion is observed. Phase transitions in the resulting coordination compounds are studied by differential scanning calorimetry and optical polarizing thermomicroscopy. The presence of several polymorphic crystalline modifications, as well as mesophases, is established. Mesomorphic properties are found for complexes with chloride and tetrafluoroborate anions.

**DOI:** 10.1134/S0022476616030094

**Keywords:** iron(III) complexes, Schiff base, structure, mass spectrometry, mesomorphism.

## INTRODUCTION

The development of new types of ligand systems has been a crucial step in the chemistry of metal complexes with physicochemical properties essential for scientific research and practical applications. The compounds particularly important as ligands are Schiff bases (azomethines and imines) and their structural analogues, i.e., compounds containing  $\text{-N=CH}$  bonds (imino group) [1] because of a wide variability of the resulting ligand structures (depending on the selected aldehyde and amine), their easy bonding with metals, and their diverse applications [2, 3]. There is a keen interest in studying dendrimers, i.e., new mesogenic structures with a large internal free volume, which allows one to expand the applications of liquid crystal materials [4]. In terms of potential applications, the combination of dendrimer properties with the specific properties of transition metal ions is highly promising. The metal ion in metal dendrimers acts as a structural unit and can be integrated in different ways: into the dendrimer core [5], as metal complexes that have coordination bonds with the dendrimer periphery [6], or as periphery units at the branching points of the dendrimer branches [7]. The main areas of research on the physical properties of metal dendrimers are focused on catalysis [8], light absorption and luminescence properties [9], electrochemical behavior, sensor, magnetic, and spin dependent properties [10, 11], and nanoobjects in medicine [12]. Here

---

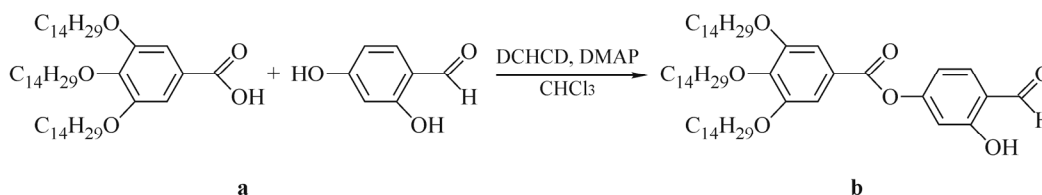
<sup>1</sup>Krestov Institute of Solution Chemistry, Russian Academy of Sciences, Ivanovo, Russia; uch@isc-ras.ru. <sup>2</sup>Ivanovo State University, Ivanovo, Russia. Translated from *Zhurnal Strukturnoi Khimii*, Vol. 57, No. 3, pp. 506-519, March-April, 2016. Original article submitted February 12, 2015.

we should mention the works where a ferrous iron is coordinated to a nitrogen-containing ligand [13, 14] to obtain liquid crystal Fe(II) complexes demonstrating spin dependent properties, as a vivid example of polyfunctional materials and organometallic networks.

The aim of our study was to synthesize a series of metal complexes with a dendrimer periphery, determine their purity and structure by a number of modern physicochemical analysis techniques, and establish a relationship between the structure and the manifested phase transitions and supramolecular structures. Previously, researchers have investigated the temperature-dependent magnetic properties of iron(III) bis[3,4,5-tri(tetradecyloxy)benzoyloxybenzoyl-4-oxy-salicylidene-N'-ethyl-N-ethylenediamine]nitrate (**1**) [15]. They have found that the iron(III) ion in the octahedral coordination node is in a high-spin state at room temperature. At lower temperatures, the sample becomes magnetically ordered. This situation is typical of the antiferromagnetic-type ordering in complexes with a dimer supramolecular architecture and the high-spin state of the central ion [16]. Thus, they showed a solution for the problem of molecular design of coordination compounds in which liquid crystal phase transitions largely affect the spin-dependent behavior of the central magnetic ion.

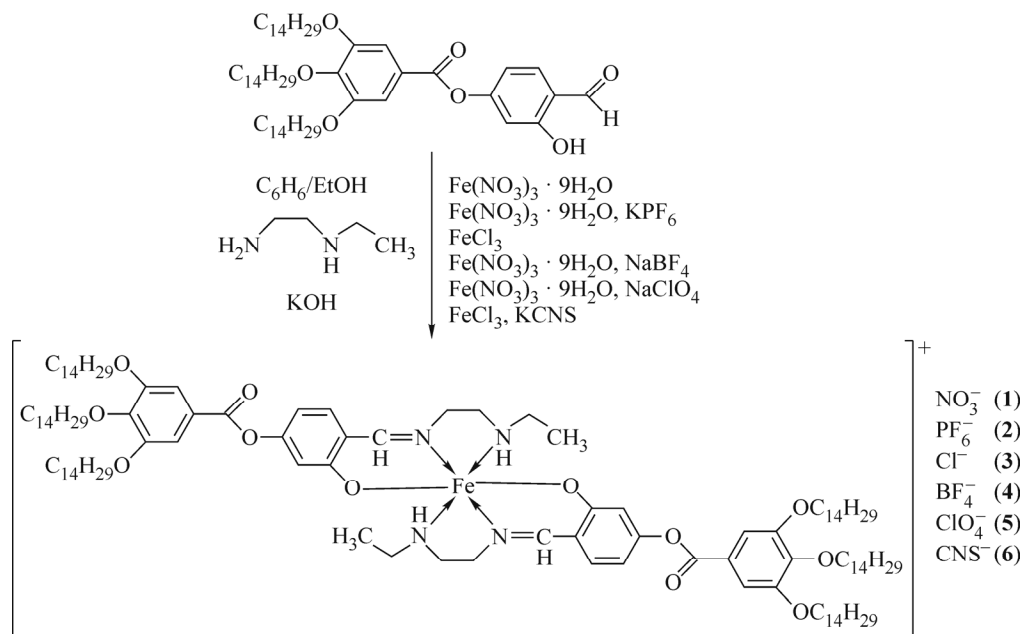
## EXPERIMENTAL

All the reagents and solvents had the CP grade and were not further purified. The synthesis of 3,4,5-tri(tetradecyloxy)benzoyloxy-2-hydroxybenzaldehyde was performed according to Scheme 1 by forming an ester bond with *m*-hydroxy-salicylic aldehyde, in a similar way as in [17].



Scheme 1. Synthesis of 3,4,5-tri(tetradecyloxy)benzoyloxy-2-hydroxybenzaldehyde.

The target compounds were synthesized according to Scheme 2 in a benzene/ethanol binary solvent [18, 19]; the use of this solvent enables better dissolution of the initial reagents and a fuller complexation reaction. Azomethine was obtained



Scheme 2. Synthesis of the iron(III) complexes.

directly in the solution between 3,4,5-tri(tetradecyloxy)benzoyloxy-2-hydrobenzaldehyde and N'-ethyl-N-ethylenediamine in the presence of KOH, which accelerates the reaction. The complexation process occurred when the iron(III) salt was added. The counterion was substituted by adding a double excess of the corresponding potassium or sodium salts.

The synthesized compounds were characterized in terms of purity, individuality, and physicochemical properties by the methods described below.

**The infrared (IR) spectra** of the compounds were recorded using a Bruker Vertex 80V device in the range 7500-370  $\text{cm}^{-1}$  and 670-190  $\text{cm}^{-1}$  in KBr and CsBr pellets.  $^1\text{H}$  (500.17 MHz) and  $^{13}\text{C}$  (125.76 MHz) NMR spectra were recorded on a Bruker Avance-500 device, using tetramethylsilane as the internal standard. The elemental analysis of the solid compounds was performed using a FlashEA 1112 analyzer for C, H, N, and O. Gel exclusion chromatography was performed on a Shimadzu 10A liquid chromatographer with a two-channel UV detector and a diffractometer, using tetrahydrofuran as an eluent. The electron absorption spectra (EAS) were recorded on a Cary-100 Varian spectrophotometer in 10-mm thick cuvettes. The mass spectra were recorded using an Ultraflex III Bruker with a time-of-flight mass analyzer; the spectra were recorded in a positive-ion mode. The samples were applied onto the target in the following matrices: 2,5-dihydroxy benzoic acid (DHB) and *n*-nitroaniline (PNA). The phase transitions in the samples were studied using a Min-8 polarization microscope equipped with a warm stage and a microphoto attachment. The DSC curves were recorded using a DSC 204 F1 Phoenix differential scanning calorimeter with a  $\mu$ -sensor (NETZSCH). The scanning rate during heating and cooling was 10 K/min in an argon atmosphere.

Similar synthesis techniques and spectral characteristics of original 3,4,5-tri(tetradecyloxy)benzoyloxy-2-hydrobenzaldehyde and the complexes are given in Appendix.

## APPENDIX

**3,4,5-Tris(tetradecyloxy)benzoic acid (a).** Weighed portions of tetradecyl bromide (20.22 g) and ethyl ether of 3,4,5-trihydroxybenzoic acid (4.89 g) were dissolved in 200 ml acetone. Then 4% NaOH in  $\text{C}_2\text{H}_5\text{OH}$  was added and boiled for 8 h. We monitored the reaction using thin layer chromatography. Then the mixture was poured in a 1 M HCl solution, the solid precipitate was filtered, and the solvent was evaporated. In chromatography  $\text{Al}_2\text{O}_3$  was used with diethyl ester as an eluent. The solvent was distilled off. The yield: 15 g (80%). Found, %: C 76.78, H 14.52, O 10.63.  $\text{C}_{49}\text{H}_{90}\text{O}_5$ . Calculated, %: C 77.52, H 11.95, O 10.54. MS (MALDI-ToF): *m/z*: found 781.94; calculated 782.25 [ $\text{M}^+\text{Na}$ ]. IR spectrum,  $\nu$ ,  $\text{cm}^{-1}$ : 4326, 4250 (m, intermolecular hydrogen bond), 3418 (w, OH vibrations), 3081 (w, aromatic C-H vibrations), 2921-2850 (s,  $-\text{CH}_2$  vibrations), 2637-2530 (m,  $-\text{CH}_3$  vibrations), 1688 (s, C=O vibrations), 1130 (w,  $-\text{C}-\text{O}-\text{C}-$ ), 989-969 (m, planar bending C-H vibrations of a 1,3,4,5-substituted aromatic ring), 936 (w, OH vibrations), and 866 (s, nonplanar bending C-H vibrations of a 1,3,4,5-substituted aromatic ring).  $^1\text{H}$  NMR spectrum ( $\text{CDCl}_3$ , TMS)  $\delta$ , ppm: 0.81 (t, 9H,  $\text{CH}_3$ -Alk,  $J = 7.324$  Hz); 1.19 (m, 54H,  $-\text{CH}_2$ -Alk,  $J = 44.556$  Hz); 1.41 (t, 6H, Alk- $\text{CH}_2$ - $\text{CH}_2$ -O-,  $J = 6.714$  Hz); 1.68 (m, 6H,  $-\text{CH}_2$ -Alk,  $J = 7.324$  Hz); 1.75 (m, 6H,  $-\text{CH}_2$ -Alk,  $J = 7.935$  Hz); 3.95 (m, 6H, Alk- $\text{CH}_2$ -O,  $J = 6.104$  Hz); 7.19 (s, 2H, Ph-H); and 11.98 (s, 1H, COOH). The  $^{13}\text{C}$  NMR spectrum ( $\text{CDCl}_3$ , TMS)  $\delta$ , ppm: 14.11 ( $\text{CH}_3$ -), 22.69 ( $\text{CH}_3$ - $\text{CH}_2$ -), 26.06 ( $\text{CH}_3$ - $\text{CH}_2$ - $\text{CH}_2$ -), 29.70 ( $\text{CH}_2$ -Alk), 31.92 ( $\text{O}-\text{CH}_2$ - $\text{CH}_2$ - $\text{CH}_2$ -), 69.14 ( $\text{O}-\text{CH}_2$ -Alk), 73.52 ( $\text{O}-\text{CH}_2$ - $\text{CH}_2$ -), 108.47 ( $\text{CH}_{\text{arom}}$ ), 123.58 ( $\text{C}_{\text{arom}}$ ), 143.10 ( $\text{C}_{\text{arom}}$ ), 152.82 ( $\text{C}_{\text{arom}}$ ), and 171.87 (C(O)OH).

**3,4,5-Tri(tetradecyloxy)benzoyloxy-2-hydroxybenzaldehyde (b).** A weighed portion of 3,4,5-tris(tetradecyloxy)benzoic acid (6 g; 7.9 mmol) was dissolved in chloroform. Then 2,4-dihydrobenzaldehyde (1.09 g; 7.9 mmol) was added and stirred until complete dissolution. Then a weighed portion of dicyclohexylcarbodiimide (DCHCD) (2.25 g; 10.9 mmol) was added and stirred for 30 min. Then a catalytic amount of dimethylaminopyridine (DMAP) was added and kept stirring for 12 h. A part of the solvent was distilled off. We used silica gel chromatography with chloroform as an eluent. The substance was lyophilized from benzene. Yield: 5.6 g (80.6%). Found, %: C 75.93, H 11.17, O 12.70.  $\text{C}_{56}\text{H}_{94}\text{O}_7$ . Calculated, %: C 76.49, H 10.77, O 12.74. MS (MALDI-ToF): *m/z*: found 902.33; calculated 902.36 [ $\text{M}^+\text{Na}$ ]. IR spectrum,  $\nu$ ,  $\text{cm}^{-1}$ : 4329, 4253 (w, intermolecular hydrogen bond), 3433 (w, OH vibrations), 3091 (w, aromatic CH vibrations), 2919-2848 (s,  $-\text{CH}_2$  vibrations), 1727 (s, C=O vibrations), 1617 (s, Ph-OH of salicylic aldehyde), 1386-1274 (s, Ph-CHO), 1193 (s, Alk-C-O-C(Ph)), 982 (m, planar bending C-H vibrations of a 1,3,4,5-substituted aromatic ring), and 873

(w, OH vibrations). The  $^1\text{H}$  NMR spectrum ( $\text{CDCl}_3$ , TMS)  $\delta$ , ppm: 0.81 (t, 9H,  $\text{CH}_3$ -,  $J = 6.104$  Hz); 1.28-1.19 (m, 54H,  $-\text{CH}_2$ -Alk,  $J = 49.438$  Hz); 1.41 (t, 6H, Alk- $\text{CH}_2$ - $\text{CH}_2$ -O-,  $J = 6.104$  Hz); 1.69 (m, 6H,  $-\text{CH}_2$ -Alk,  $J = 6.714$  Hz); 1.76 (m, 6H,  $-\text{CH}_2$ -Alk,  $J = 6.714$  Hz); 3.97 (m, 6H, Alk- $\text{CH}_2$ -O,  $J = 6.104$  Hz); 6.83-6.79 (d, 2H, Ph-H,  $J = 7.935$  Hz); 7.19 (s, 1H, Ph-H); 7.56-7.54 (d, 2H, Ph-H,  $J = 8.545$  Hz); 9.82 (s, 1H, OH-); 11.19 (c, 1H, COH). The  $^{13}\text{C}$  NMR spectrum ( $\text{CDCl}_3$ , TMS)  $\delta$ , ppm: 14.15 ( $\text{CH}_3$ -), 22.72 ( $\text{CH}_3$ - $\text{CH}_2$ -), 26.09 ( $-\text{CH}_2$ -), 29.41 ( $-\text{CH}_2$ -), 29.72 ( $-\text{CH}_2$ -), 29.74 ( $-\text{CH}_2$ -), 30.37 ( $-\text{CH}_2$ -), 31.96 ( $\text{CH}_3$ - $\text{CH}_2$ - $\text{CH}_2$ -), 69.30 ( $-\text{O}-\text{CH}_2$ -Alk), 73.64 ( $-\text{O}-\text{CH}_2$ -Alk), 108.64 ( $\text{CH}_{\text{arom}}$ ), 110.98 ( $\text{CH}_{\text{arom}}$ ), 114.18 ( $\text{CH}_{\text{arom}}$ ), 118.69 ( $\text{C}_{\text{arom}}$ ), 123.06 ( $\text{C}_{\text{arom}}$ ), 134.97 ( $\text{CH}_{\text{arom}}$ ), 143.39 ( $\text{C}_{\text{arom}}$ ), 153.04 ( $\text{C}_{\text{arom}}$ ), 157.82 ( $\text{C}_{\text{arom}}$ ), 163.21 ( $\text{C}_{\text{arom}}-\text{OH}$ ), 164.06 ( $\text{C}(\text{O})\text{O}$ ), and 195.52 (CHO).

**Bis[3,4,5-tri(tetradecyloxy)benzoyloxybenzoyl-4-oxy-salicylidene-N'-ethyl-N-ethylenediamine]iron(III) nitrate (1).** A weighed portion of 3,4,5-tri(tetradecyloxy)-benzoyloxy-2-hydroxybenzaldehyde (0.9 g) was dissolved in benzene (6 ml). Then we added N'-ethyl-N-ethylenediamine (0.09 g) dissolved in ethyl alcohol (10 ml), stirred for 5 min, and added an alcohol solution of KOH (0.113 g, 10 ml). A  $\text{Fe}(\text{NO}_3)_3 \cdot 9\text{H}_2\text{O}$  solution (0.21 g) in ethanol was added slowly, dropwise, to the mixture. The resulting mixture was stirred for 2 h, filtered with a fine glass filter, and washed with ethyl alcohol. The product was reprecipitated from a mixture of dried benzene-ethanol (1/6) solvents with the subsequent lyophilization from benzene. The product was a fine dark brown powder. Yield: 1.02 g. Found, %: C 70.71, H 11.44, N 3.29, O 10.83.  $\text{C}_{120}\text{H}_{206}\text{N}_4\text{O}_{12}\text{FeNO}_3$ . Calculated, %: C 71.53, H 10.30, N 3.47, O 11.91. IR spectrum,  $\nu$ ,  $\text{cm}^{-1}$ : 3182.81 (w, aromatic, stretching C-H vibrations), 2927.26, 2852.52 (s,  $-(\text{CH}_2)_n-\text{CH}_3$ ), 1734.71 (s, C=O), 1635.46 (s, C=N), 1384.23 (s,  $\text{NO}_3^-$  vibrations), 1193.75, 1120.03 (s, Alk-C-O-C(Ph)), 990.41 (m, NH vibrations), 864.73, 824.91 (s, symmetric vibrations of the 1,4-disubstituted aromatic ring).

**Bis[3,4,5-tri(tetradecyloxy)benzoyloxybenzoyl-4-oxy-salicylidene-N'-ethyl-N-ethylenediamine]iron(III) hexafluorophosphate (2).** The synthesis was similar to that of complex (1). In 15 min after adding an alcohol solution of  $\text{Fe}(\text{NO}_3)_3 \cdot 9\text{H}_2\text{O}$  (0.21 g), we added a weighed portion of  $\text{KPF}_6$  (0.37 g) dissolved in ethanol with several drops of water. The synthesis continued for 4 h. The precipitate was filtered with a glass filter and reprecipitated from the mixture of dried benzene-ethanol solvents (1/6) with the subsequent lyophilization from benzene. The product was a fine solid dark brown powder. Yield: 1.11 g. Found, %: C 69.04, H 9.60, N 3.09, O 9.87.  $\text{C}_{120}\text{H}_{206}\text{N}_4\text{O}_{12}\text{FePF}_6$ . Calculated, %: C 68.70, H 9.89, N 2.67, O 9.15. The IR spectrum,  $\nu$ ,  $\text{cm}^{-1}$ : 3209.91, 3119.28 (w, aromatic, stretching C-H vibrations), 2916.70, 2849.18 (s,  $-(\text{CH}_2)_n-\text{CH}_3$ ), 1736.78 (s, C=O), 1626.17 (s, C=N), 1192.36, 1121.72 (s, Alk-C-O-C(Ph)), 989.12 (m, NH vibrations), and 845.18 (w,  $\text{PF}_6^-$  vibrations).

**Bis[3,4,5-tri(tetradecyloxy)benzoyloxybenzoyl-4-oxy-salicylidene-N'-ethyl-N-ethylenediamine]iron(III) chloride (3).** The synthesis was similar to that of complex (1). After adding an alcohol solution of KOH (0.113 g, 10 ml), we added slowly, dropwise, a solution of  $\text{FeCl}_3$  (0.083 g) in ethanol, stirred for 2 h, filtered with a glass filter, washed with ethyl alcohol, and reprecipitated from a mixture of dried benzene-ethanol (1/6) solvents with the subsequent lyophilization from benzene. The product was a fine solid dark brown powder. Yield: 0.89 g. Found, %: C 71.58, H 10.79, N 2.32, O 9.60.  $\text{C}_{120}\text{H}_{206}\text{N}_4\text{O}_{12}\text{FeCl}$ . Calculated, %: C 72.49, H 10.44, N 2.82, O 9.66. IR spectrum,  $\nu$ ,  $\text{cm}^{-1}$ : 3078.75 (w, aromatic, stretching C-H vibrations), 2920.26, 2852.29 (s,  $-(\text{CH}_2)_n-\text{CH}_3$ ), 1730.12 (s, C=O), 1630.16 (s, C=N), 1191.69, 1118.42 (s, Alk-C-O-C(Ph)), 988.05 (s, NH-vibrations), and 544.60 (w,  $\text{Cl}^-$  vibrations).

**Bis[3,4,5-tri(tetradecyloxy)benzoyloxybenzoyl-4-oxy-salicylidene-N'-ethyl-N-ethylenediamine]iron(III) tetrafluoroborate (4).** The synthesis was similar to that of complex (1). In 15 min after adding an alcohol solution of  $\text{Fe}(\text{NO}_3)_3 \cdot 9\text{H}_2\text{O}$  (0.21 g), we added a weighed portion of  $\text{NaBF}_4$  (0.22 g) dissolved in several drops of water. The reaction continued for 6 h, and the reaction mass was kept for 12 h in a refrigerator. The solution was filtered with a glass filter, washed with ethyl alcohol, and reprecipitated from a mixture of dried benzene-ethanol (1/6) solvents with the subsequent lyophilization from benzene. The product was a fine solid dark brown powder. Yield: 1.03 g. Found, %: C 71.04, H 9.72, N 3.15, O 11.01.  $\text{C}_{120}\text{H}_{206}\text{N}_4\text{O}_{12}\text{FeBF}_4$ . Calculated, %: C 70.66, H 10.18, N 2.75, O 9.41. IR spectrum,  $\nu$ ,  $\text{cm}^{-1}$ : 3182.81, 3064.19 (w, aromatic, stretching C-H vibrations), 2921.59, 2848.29 (s,  $-(\text{CH}_2)_n-\text{CH}_3$ ), 1716.79 (s, C=O), 1624.83 (m, C=N), 1213.02, 1190.36, 1111.73 (s, Alk-C-O-C(Ph)), 1033.09 (s,  $\text{BF}_4^-$  vibrations), and 987.78 (m, NH vibrations).

**Bis[3,4,5-tri(tetradecyloxy)benzoyloxybenzoyl-4-oxy-salicylidene-N'-ethyl-N-ethylenediamine]iron(III) perchlorate (5).** The synthesis was similar to that of complex (1). In 15 min after adding an alcohol solution of  $\text{Fe}(\text{NO}_3)_3 \cdot 9\text{H}_2\text{O}$  (0.21 g), we added a weighed portion of  $\text{NaClO}_4$  (0.249 g) dissolved in ethanol. The synthesis continued for 4 h. The precipitate was filtered with a glass filter, washed with ethyl alcohol, reprecipitated from a mixture of dried benzene–ethanol (1/6) solvents with the subsequent lyophilization from benzene. The product was a fine solid dark brown powder. Yield: 1.05 g. Found, %: C 69.86, H 9.50, N 2.14, O 13.67.  $\text{C}_{120}\text{H}_{206}\text{N}_4\text{O}_{12}\text{FeClO}_4$ . Calculated, %: C 70.29, H 10.03, N 2.73, O 12.48. IR spectrum,  $\nu$ ,  $\text{cm}^{-1}$ : 3200.79 (m, aromatic, stretching C–H vibrations), 2917.81, 2852.51 (s,  $-(\text{CH}_2)_n-\text{CH}_3$ ), 1733.01 (s, C=O), 1628.83 (s, C=N), 1193.47 (s, Alk–C–O–C(Ph)), 1115.73 (s,  $\text{ClO}_4^-$  vibrations), and 989.78 (m, NH vibrations).

**Bis[3,4,5-tri(tetradecyloxy)benzoyloxybenzoyl-4-oxy-salicylidene-N'-ethyl-N-ethylenediamine]iron(III) thiocyanate (6).** The synthesis was similar to that of complex (3). In 10 min after adding an alcohol solution of  $\text{FeCl}_3$  (0.053 g), we added a weighed portion of KCNS (0.129 g) dissolved in ethanol. The synthesis continued for 4 h. Then we kept the reaction mass in a refrigerator for one day. The precipitate was filtered with a glass filter, washed with ethyl alcohol, reprecipitated from a mixture of dried benzene–ethanol (1/6) solvents with the subsequent lyophilization from benzene. The product was a fine solid dark brown powder. Yield: 0.59 g. Found, %: C 71.43, H 9.78, N 2.99, O 9.01, S 2.03.  $\text{C}_{120}\text{H}_{206}\text{N}_4\text{O}_{12}\text{FeCNS}$ . Calculated, %: C 72.27, H 10.32, N 3.48, O 9.55, S 1.59. IR spectrum,  $\nu$ ,  $\text{cm}^{-1}$ : 3067.56 (w, aromatic, stretching C–H vibrations), 2920.16, 2849.25 (s,  $-(\text{CH}_2)_n-\text{CH}_3$ ), 2044.15 (s,  $\text{CNS}^-$  vibrations), 1714.61 (s, C=O), 1585.29 (s, C=N), 1214.03, 1108.35 (s, Alk–C–O–C(Ph)), and 997.11 (m, NH vibrations).

The preparation of single crystals from concentrated solutions of the synthesized compounds did not give the desired result, which was likely due to the presence of a large number of long alkyl chains.

## RESULTS AND DISCUSSION

In order to confirm the structure and purity of the synthesized oligomeric compounds, we conducted a chromatographic analysis and recorded the electron, IR, NMR, and mass spectra of the samples.

**UV spectroscopy.** Since the complexation process involves the sedimentation of the desired product in the form of a fine powder which may be contaminated with the original iron-containing salt, it was necessary to determine the purity of the chelate compounds. The literature describes applications of electron spectroscopy to identify additions of original substances in the target compound [20]. The electron absorption spectra were recorded in a dichloromethane solution. As seen from the electron spectrum of (1) and its comparison with the original salt  $\text{Fe}(\text{NO}_3)_3 \cdot 9\text{H}_2\text{O}$ , the resulting compound has no traces of unreacted salts after the sedimentation and additional lyophilization (Fig. 1).

The analysis of the experimental data allows us to conclude that there are no unreacted  $\text{Fe}(\text{NO}_3)_3 \cdot 9\text{H}_2\text{O}$  and  $\text{FeCl}_3$  salts. The spectra of all the complexes, except (6), demonstrate four bands. The high-energy band at 227–228 nm is

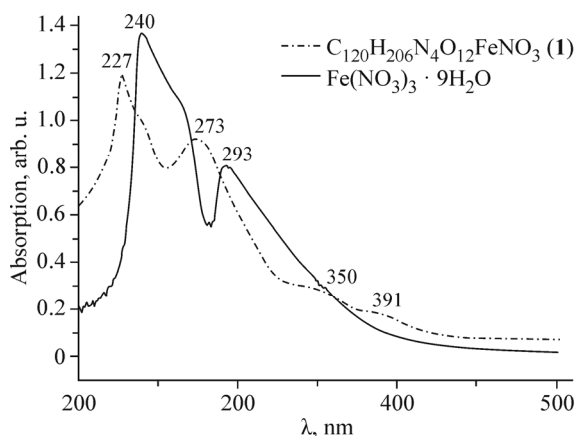


**Fig. 1.** UV spectra of complex 1 and  $\text{Fe}(\text{NO}_3)_3 \cdot 9\text{H}_2\text{O}$ .

**TABLE 1.** Positions of the Maxima of the Electron Absorption Bands and Relative Absorption Coefficients (in parentheses) at the Band Maxima for Complexes **1-6** and the Original Salts

No.	Compound	$\lambda_1$ , nm	$\lambda_2$ , nm	$\lambda_3$ , nm	$\lambda_4$ , nm	No.	Compound	$\lambda_1$ , nm	$\lambda_2$ , nm	$\lambda_3$ , nm	$\lambda_4$ , nm
<b>1</b>	$C_{120}H_{206}N_4O_{12}FeNO_3$	227 (1.19)	273 (0.92)	350 (0.28)	391 (0.17)	<b>5</b>	$C_{120}H_{206}N_4O_{12}FeClO_4$	228 (1.62)	274 (1.26)	348 (0.34)	394 (0.18)
<b>2</b>	$C_{120}H_{206}N_4O_{12}FePF_6$	227 (1.41)	275 (1.09)	349 (0.29)	393 (0.14)	<b>6</b>	$C_{120}H_{206}N_4O_{12}FeCNS$	228 (0.64)	268 (0.74)	–	–
<b>3</b>	$C_{120}H_{206}N_4O_{12}FeCl$	228 (2.04)	271 (1.83)	350 (0.38)	393 (0.23)		$Fe(NO_3)_3 \cdot 9H_2O$	240 (1.37)	293 (0.81)	–	–
<b>4</b>	$C_{120}H_{206}N_4O_{12}FeBF_4$	227 (0.83)	270 (0.74)	351 (0.14)	392 (0.08)		$FeCl_3$	249 (2.11)	329 (1.51)	361 (1.75)	–

responsible for the excitation of  $\pi$  electrons ( $\pi-\pi^*$  transitions) of the aromatic rings. The band at 273-268 nm corresponds to the intramolecular  $n-\pi^*$  transitions of the conjugated aromatic systems. The band at 349-351 nm is associated with the  $\pi-\pi^*$  transition of the chromophore of the Schiff base ( $CH=N$ ) [21, 22]. The weak band at 391-394 nm characterizes the intramolecular energy transfer from  $p$  electrons of the donor atomic  $\pi$  orbitals of the ligand to the  $d$  metal orbitals [23, 24]. The characteristic bands of the transitions are given in Table 1.

**Chromatographic analysis.** The chemical purity and homogeneity of metal chelates **1-6** were also analyzed by gel exclusion chromatography; the samples were eluted with dry tetrahydrofuran. 1,2-dichlorobenzene was used as the standard. Fig. 2 shows, as an example, the chromatograms of the complexes with tetrafluoroborate **4** and thiocyanate **6** ions. The eluting time is  $\tau_2$ .

The chromatograms of the coordination compounds have low-intensity peaks ( $\tau_1$ ) typical of aggregates with a high molecular mass [25, 26]. The parameters of the chromatographic distribution of compounds **1-6** are given in Table 2.

A substantial contribution to the polydispersity of the sample comes from the impact of the counterion. The higher the hydrogen-bonding capacity of the counterion, the higher the polydispersity index of the compound, which may explain

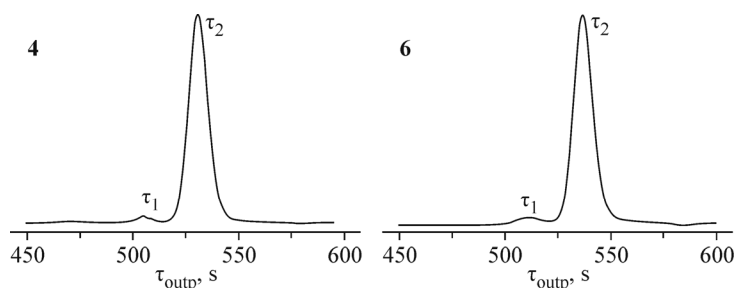


**Fig. 2.** Chromatograms of complexes **4** and **6**.

**TABLE 2.** Parameters of the Chromatographic Distribution of Compounds **1-6**

No.	Compound	$M$	$\tau_{2st}$	$\tau_{2end}$	$P_i$	$P_z$
<b>1</b>	$C_{120}H_{206}N_4O_{12}FeNO_3$	2014.93	8.69	9.19	1.038	1.037
<b>2</b>	$C_{120}H_{206}N_4O_{12}FePF_6$	2097.90	8.71	9.40	1.040	1.035
<b>3</b>	$C_{120}H_{206}N_4O_{12}FeCl$	1988.43	8.65	9.42	1.047	1.039
<b>4</b>	$C_{120}H_{206}N_4O_{12}FeBF_4$	2039.75	8.65	9.36	1.025	1.024
<b>5</b>	$C_{120}H_{206}N_4O_{12}FeClO_4$	2050.37	8.74	9.42	1.038	1.033
<b>6</b>	$C_{120}H_{206}N_4O_{12}FeCNS$	2011.02	8.71	9.31	1.026	1.024

$P_i$  is the polydispersity index;  $P_z$  is the ratio between the retained volume  $V_r$  and the molecular mass  $M$ .

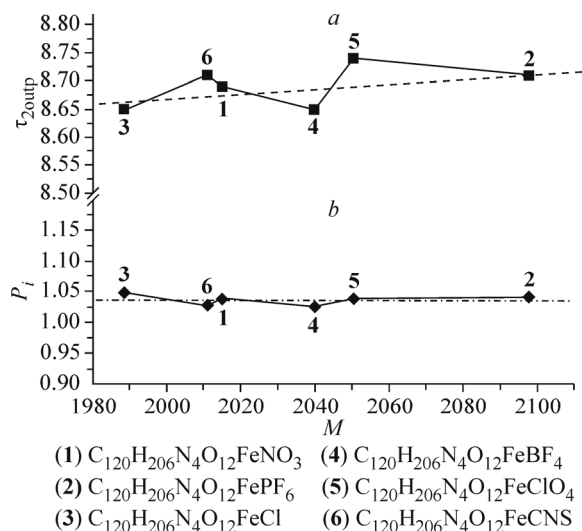


**Fig. 3.** Dependence of the output time  $\tau_{2out}$  of the complex on molecular mass (a); dependence of the polydispersity index  $P_i$  on the molecular mass of the complex (b).

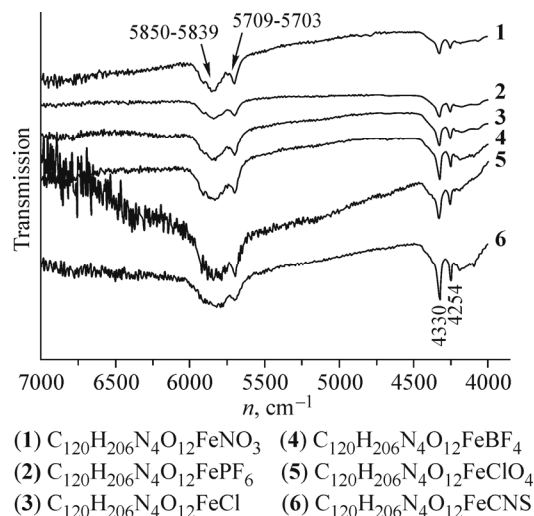


**Fig. 4.** IR spectra of the complexes at 7000-4000  $cm^{-1}$ .

the nature of the formation of aggregates ( $\tau_1$ ) by the complexes. This is confirmed by the mass spectrometry and IR spectroscopy data. The linear dependence of  $\tau_{2out}$  on the molecular weight indicates the identity of the entire homological series to the one being analyzed (Fig. 3).

**NMR spectroscopy.** The  $^1H$  NMR spectra of the complexes have two series of broadened signals in weak (7-8 pbw) and strong (0.5-4 pbw) fields, which gives evidence of the paramagnetic nature of the samples, i.e., the effect of the metal ion on the proton vibrations in the azomethine molecule. Such a dramatic shift, i.e., a broadening in the absence of signal multiplicity in the NMR spectra of coordination compounds with paramagnetic metal ions, is typical and consistent with the data in [27].

**IR spectroscopy.** The IR spectroscopy studies of the samples revealed the presence of a Schiff base and coordinated Fe(III) ion in the structure of the complexes. The bands at 5850-5839  $cm^{-1}$  and 5709-5703  $cm^{-1}$  correspond to the vibrations of two amines: tertiary and secondary respectively (Fig. 4) [28].

The range 3400-2600  $cm^{-1}$  is dominated by the 2924-2831  $cm^{-1}$  bands associated with the stretching vibrations of the alkyl and methyl fragments. The  $\nu_{H-Ph}$  proton vibrations in the aromatic rings at 3226-3185  $cm^{-1}$  have a low intensity and are substantially broadened due to the screening of the alkyl chain vibrations. The formation of the  $-CH=N-$  azomethine bond is evidenced by the vibrational band at  $\sim 1625$   $cm^{-1}$ , which is located near the vibrational band of the carboxyl group  $C=O$  (1736-1732  $cm^{-1}$ ), Fig. 5 [29, 30].

In the series of complexes **1** to **6**, there is a shift and splitting of the  $C=O$  group vibrational band from 1736-1732  $cm^{-1}$  to 1716  $cm^{-1}$  and 1706  $cm^{-1}$ . These band positions may be attributed to the interaction between the cation part of the complex and the anion. The vibrational band of the  $CH=N$  azomethine bond (1635-1625  $cm^{-1}$ ) is observed to attenuate. The bands at 1583  $cm^{-1}$  and 1539  $cm^{-1}$  demonstrate a symmetric coordination of the  $Fe^{3+}$  ions with two ligand molecules, suggesting that the metal is coordinated via the nitrogen atoms of the azomethine group [31-33]. The fact that the spectra of the complexes have no vibrational band associated with the  $Ph-OH$  fragment of salicylic aldehyde at 1617  $cm^{-1}$  indicates that the metal is coordinated via the deprotonated phenol group ( $Ph-O^-$ ) located near the azomethine moiety.

The IR spectra of each complex are observed to have absorption bands typical of the vibration of the counterions (Fig. 6). These are 825  $cm^{-1}$  and a broadened signal at  $\sim 1384$   $cm^{-1}$  for the nitrate ion (**1**), an intense signal at  $\sim 846$   $cm^{-1}$  and 558  $cm^{-1}$  for the hexafluorophosphate ion (**2**),  $\sim 544$   $cm^{-1}$  for the chloride ion (**3**),  $\sim 1033$   $cm^{-1}$ , 539  $cm^{-1}$ , and 519  $cm^{-1}$  for the tetrafluoroborate ion (**4**),  $\sim 1116$   $cm^{-1}$  and 626  $cm^{-1}$  for the perchlorate ion (**5**), and  $\sim 2044$   $cm^{-1}$  for the thiocyanate ion (**6**) [34, 35].

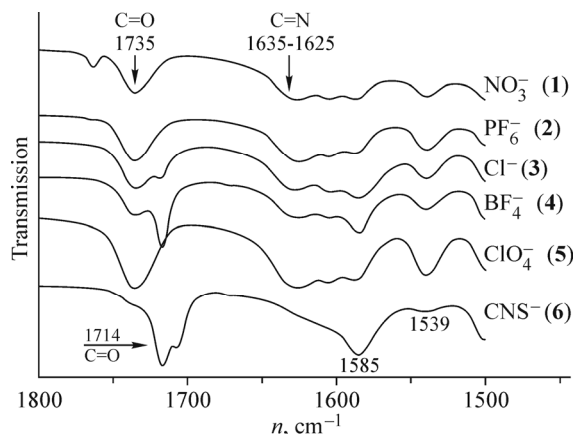


Fig. 5. IR spectra of the complexes at 1800-1500  $\text{cm}^{-1}$ .

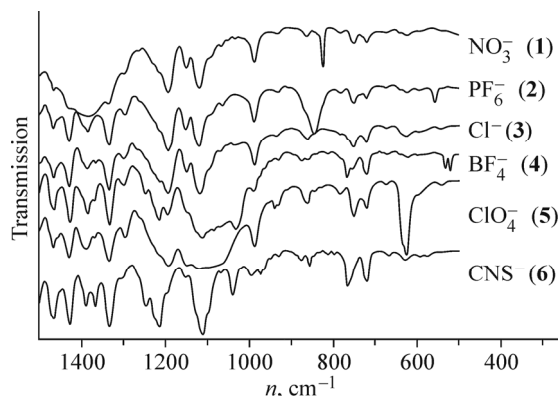


Fig. 6. IR spectra of the complexes at 1500-500  $\text{cm}^{-1}$ .

TABLE 3. Positions of the Maxima of the IR Absorption Bands for Stretching Vibrations of Fe–N and Fe–O Bonds in Complexes 1-6 in the Far Region

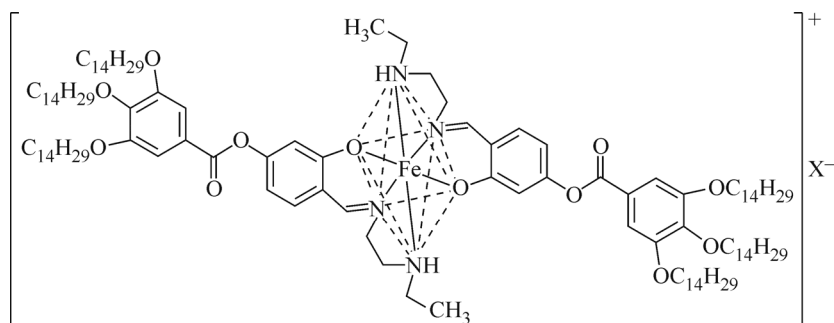
Compound	Fe–N	Fe–O	Compound	Fe–N	Fe–O
C120H206N4O12FeNO3 (1)	541	419	C120H206N4O12FeBF4 (4)	– *	419
C120H206N4O12FePF6 (2)	541	419	C120H206N4O12FeClO4 (5)	542	419
C120H206N4O12FeCl (3)	546	420	C120H206N4O12FeCNS (6)	541	417

\* Superimposition of the more intense absorption band of the  $\text{BF}_4$  counterion.

Vibrations of the bonds of the coordinated Fe(III) ion were recorded in the far region ( $690\text{--}170\text{ cm}^{-1}$ ) of the IR spectrum (Table 3) obtained in CsBr pellets [36, 37].

**Mass spectrometry.** The stability of the complexes and the presence of iron in their structure is confirmed by the mass spectrometry data [38, 39]. This method is known to be most efficient in determining the masses of heavy ions. Therefore, it is of interest to apply the method of time-of-flight mass spectrometry in combination with the results of other physicochemical methods to determine the coordination sphere of the metals. When recorded in the mode of positively charged particles, the mass spectra of the complexes contain a series of stable ions characterizing the azomethine moiety  $\sim 948\text{ a.u. }[\text{L}]^+$  and iron in its nearest environment with the composition “two ligands–iron”; i.e., there is formation of biligand systems  $[2\text{L}\cdot\text{Fe}]^+$  with a mass of  $1949\text{--}1952\text{ a.u.}$  The weak interaction of the outer sphere anion with the inner coordination sphere is manifested in the absence of stable molecular ions of the composition  $[2\text{L}\cdot\text{Fe}]^+\text{X}^-$  [40]. For all the compounds, their mass spectra clearly indicate the presence of fragment ions of the composition  $972\text{ a.u. }[\text{L}\cdot\text{Na}]^+$  and  $1004\text{ a.u. }[\text{L}\cdot\text{Fe}]^+$ , which are derived from the decay of the biligand system  $[2\cdot\text{Fe}]^+$ . It should be noted that the stability and intensity of the fragment ions relative to the fragment  $948\text{ [L]}^+$  is rather high: up to 54%, 10%, and 7%, respectively.

Based on these data, we built a structural model of the complexes, which is given, in a general form, in Scheme 3.



Scheme 3. Model of the biligand iron(III) complex,  $\text{X}^- = \text{NO}_3^-$ ,  $\text{PF}_6^-$ ,  $\text{Cl}^-$ ,  $\text{BF}_4^-$ ,  $\text{ClO}_4^-$ ,  $\text{CNS}^-$ .

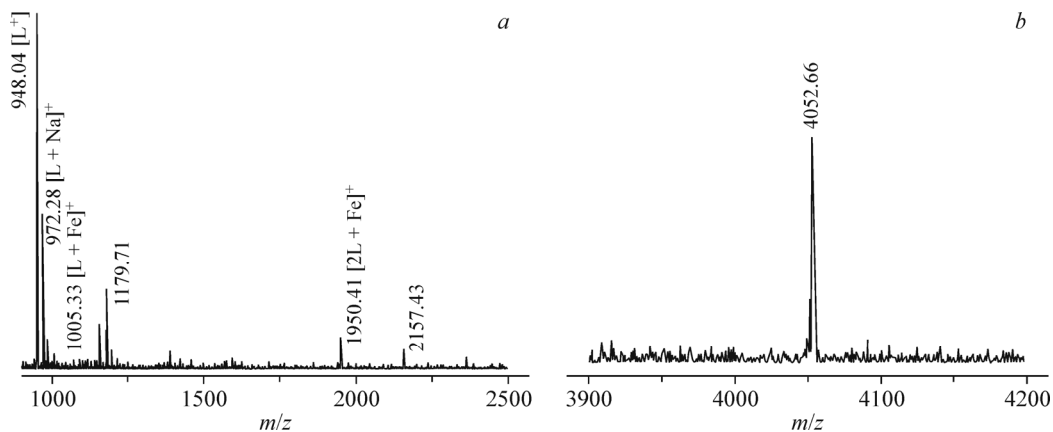
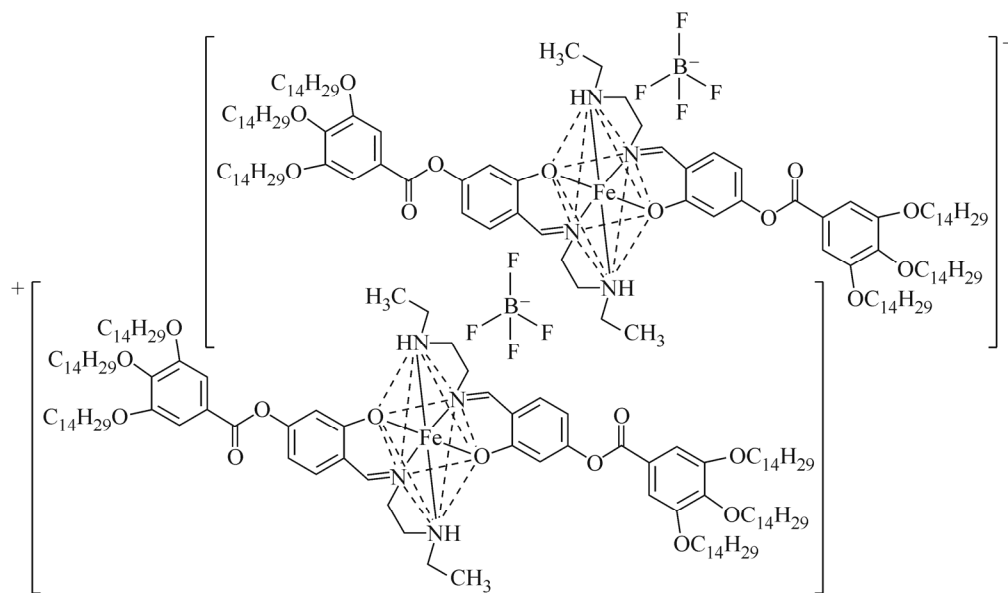


**Fig. 7.** Fragment of the mass spectrum of complex **5**, which suggests the formation of clathrate ions (*a*); fragment of the mass spectrum of complex **2**, which suggests the formation of a dimer (*b*).

The mass spectra show the presence of fairly intense clathrate ions with a molecular mass of  $\sim 2130$ ,  $2158$ , and  $2364$  of the composition  $[2L \cdot Fe]^+ +$  matrix (sinapinic acid) residue (Fig. 7*a*) [41] and dimer structures, which is evidenced by the presence of ions with a molecular mass of  $\sim 4000$ - $4200$  in the mass spectrum (Fig. 7*b*).

The dimerization process is also evidenced by peaks in the gel exclusion chromatograms  $\tau_1$  (Fig. 2), which show the output of high-molecular compounds (dimers), and a vibration band associated with strong intermolecular interactions in the near region of the IR spectra ( $4350$ - $4250$   $\text{cm}^{-1}$ ), which presumably correspond to the interaction of the counterion with the azomethine proton. Scheme 4 shows a tentative aggregation model for the complex with the tetrafluoroborate anion **4**.



Scheme 4. Formation of the dimer of complex **4**.

**Phase transitions in the complexes.** The temperature stability of complexes **1-6** was investigated from the data obtained by differential scanning calorimetry (DSC) and optical polarization thermomicroscopy. The DSC data on the temperatures and enthalpies of the phase transitions are summarized in Table 4.

According to the DSC data, complex **1** reveals several reversible solid–solid endothermic phase transitions (Fig. 8).

At negative temperatures, the compound is in the glassy state which changes to the solid-phase state with increasing temperature ( $T_{\text{melt}1} = 41.14^\circ\text{C}$ ) with a subsequent transition at  $T_{\text{melt}2} = 49.52^\circ\text{C}$ . The phase transition at a temperature of

**TABLE 4.** Phase Transition Temperatures and Changes in the Heat Capacity  $\Delta C_p$  and Enthalpy  $\Delta H$  for Complexes 1-6 in the Heating Cycle

No.	Compound	$T_g, ^\circ\text{C}$	$\Delta C_p, \text{J/g}\cdot\text{K}$	$T_{ph1}, ^\circ\text{C}$	$\Delta H, \text{J/g}$	$T_{ph2}, ^\circ\text{C}$	$\Delta H, \text{J/g}$	$T_{ph3}, ^\circ\text{C}$	$\Delta H, \text{J/g}$
1	$\text{C}_{120}\text{H}_{206}\text{N}_4\text{O}_{12}\text{FeNO}_3$	-53.12	0.58	41.14	12.46*	49.52	12.46*	144.23	17.42
2	$\text{C}_{120}\text{H}_{206}\text{N}_4\text{O}_{12}\text{FePF}_6$	–	–	10.53	1.80	40.54	22.58	139.89	4.42
3	$\text{C}_{120}\text{H}_{206}\text{N}_4\text{O}_{12}\text{FeCl}$	6.46	0.37	100.42	46.49	121.34	0.89	–	–
4	$\text{C}_{120}\text{H}_{206}\text{N}_4\text{O}_{12}\text{FeBF}_4$	–	–	48.15	76.39	–	–	–	–
5	$\text{C}_{120}\text{H}_{206}\text{N}_4\text{O}_{12}\text{FeClO}_4$	-54.29	0.31	46.02	26.20	123.10	1.20	–	–
6	$\text{C}_{120}\text{H}_{206}\text{N}_4\text{O}_{12}\text{FeCNS}$	22.36	0.17	–	–	–	–	–	–
		9.24	0.68	41.44	107.09*	46.73	107.09*	–	–

\* Total area of the peak under the curve.

$T_{\text{melt}3} = 144.23^\circ\text{C}$  can be regarded as the transition of the substance into a melt. The thermopolarization microscopy data confirm the conclusions derived from the DSC experiment, namely: at  $25^\circ\text{C}$  the substance is in the solid state and at  $54^\circ\text{C}$  there is a transition from one crystal form into another, suggesting the presence of a solid-phase transition.

The thermomicroscopic studies of complex **2** show that at temperatures above  $50^\circ\text{C}$ , the sample melts and no anisotropy is observed. The crystals are partly retained in the isotropic field up to a temperature of  $187^\circ\text{C}$  and undergo visually observable changes at about  $140^\circ\text{C}$ .

For complex **3**, the thermomicroscopy observations at a temperature of  $41^\circ\text{C}$  reveal the formation of a presumably cubic mesophase (Fig. 9) with a texture and behavior similar to that described in [42].

When heated to  $T = 45^\circ\text{C}$ , the sample changes to the isotropic state whose transition temperature differs substantially from the DSC data (Fig. 9a), which presumably suggests the formation of a cubic mesophase, since it usually has no peaks in the DSC analysis curves [43]. At  $T = 101.9^\circ\text{C}$ , the sample becomes lighter in color and the liquid becomes more viscous than that in the isotropic state; the pressing on the sample leads to birefringence. The further heating to  $T = 144.0^\circ\text{C}$  leads to increased fluidity, and the sample passes into the isotropic state. The gradual cooling of the sample to room temperature leads to the formation of finger-type domains in the glassy state (Fig. 10). The presence of these domains is typical of discotic mesogens with a hexagonal mesophase structure [44]. It is known that liquid crystals (LCs) are polymorphous. For calamitic LCs, there are examples where the substances are observed to have absolutely different phase transitions when heated and cooled [45]. There are similar examples for discotic LCs and for the related compounds – phasmids.

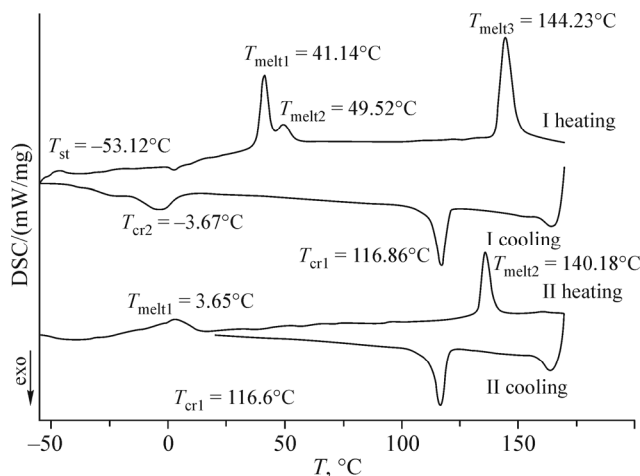


**Fig. 8.** DSC curves for complex 1.

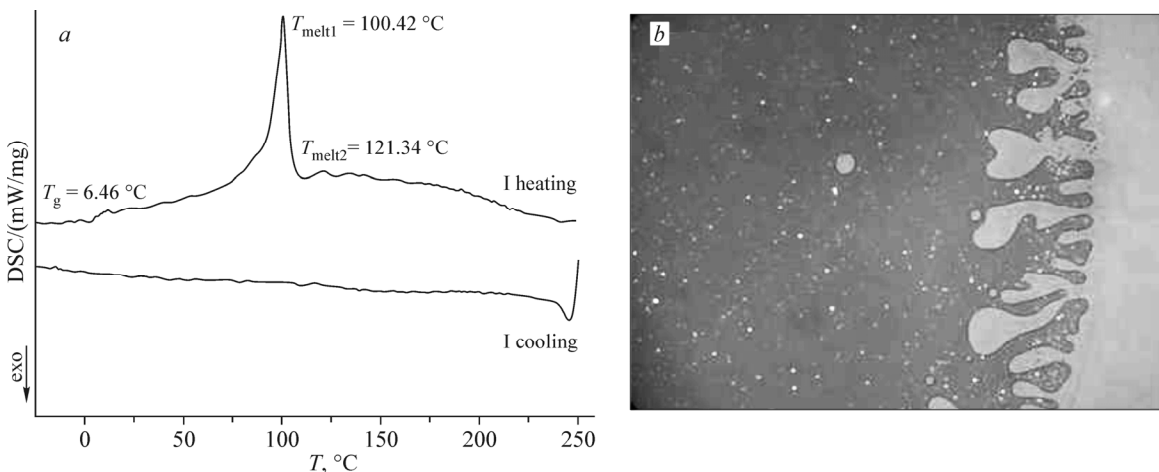


**Fig. 9.** DSC curves of complex **3** (a); crystals+cubic phase texture, heating cycle,  $T = 41,5$  °C, nicols crossed, magnification 100 (b).

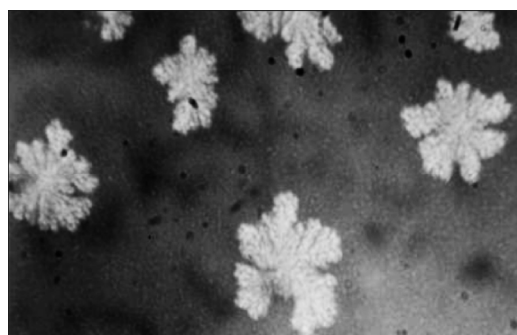


**Fig. 10.** Finger-type domains in the texture of complex **3**, cooling cycle,  $T = 25$  °C, nicols parallel, magnification 200.

In the heating cycle, complex **4** melts at a temperature of 48°C; on cooling, the sample changes from an isotropic melt to a glassy mesophase (Fig. 11) and then gradually crystallizes.

For complex **5** with the  $\text{ClO}_4^-$  counterion there is a distinct solid–solid phase transition at a temperature of 46.02°C (Table 4). The two preceding vitrification stages at  $T = -54.29$ °C and  $T = 22.36$ °C suggest that the compound is in

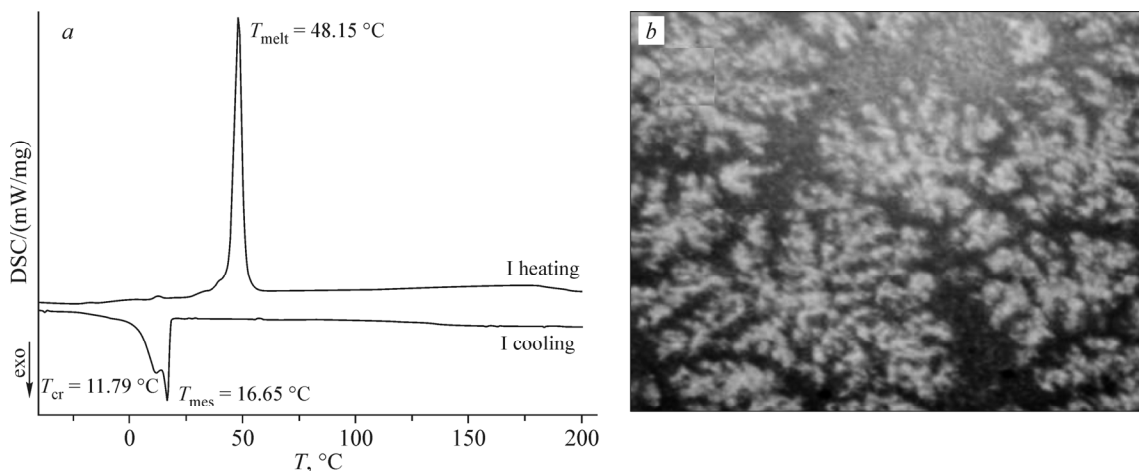


**Fig. 11.** DSC curves of complex **4** (a); vitrified mesophase texture, cooling cycle,  $T = 25$  °C, nicols parallel, magnification  $\sim 200$  (b).

a metastable glassy state, i.e., is amorphous. The melting occurs at a temperature of 123.10°C. In the cooling cycle, the sample crystallizes at a temperature of -2.57°C. The conclusions based on the DSC data are confirmed by thermopolarization microscopy. Thus, the substance melts at 120°C and remains, for a long time, in a stable melted state (mesotropic). We were able to conduct forced crystallization of the sample when it was shifted and the temperature was  $T = 60^\circ\text{C}$ , which suggests substantial supercooling of the sample and is evidence of the purity of the obtained complex.

The thermomicroscopic observations of complex **6** show that the substance melts into a brown melt at  $T = 46^\circ\text{C}$  and crystallizes into needle-like crystals when cooled.

## CONCLUSIONS

We obtained six new biligand complexes of Fe(III) based on 3,4,5-tri(tetradecyloxy)benzoyloxy-4-salicydene-N'-ethyl-N-ethylenediamine with the  $\text{NO}_3^-$  (**1**),  $\text{PF}_6^-$  (**2**),  $\text{Cl}^-$  (**3**),  $\text{BF}_4^-$  (**4**),  $\text{ClO}_4^-$  (**5**), and  $\text{CNS}^-$  (**6**) counterions. All the target compounds were characterized by a range of physicochemical methods of analysis. The presence of a complexing ion was confirmed by FT-IR spectra in the far region. The structure of the compounds was confirmed by mass spectrometric studies and elemental analysis. The formation of biligand complexes with the octahedral packing of the iron ion was observed. The study of the phase transformation in the obtained compounds revealed liquid crystal properties for the complexes with chloride and tetrafluoroborate anions. It is of interest to further examine the effect of the nature of the complexing metal on the possibility of formation of a mesophase in complexes with the same set (series) of counterions.

The spectral studies and differential scanning calorimetry used the equipment of the Upper Volga Regional Center for Physicochemical Research (Shared Resource Center).

This work was supported by the President of the Russian Federation (project No. MK-70.2014.3), RFBR (project No. 14-03-31280\_mol\_a), and Ministry of Science and Education of the Russian Federation (project No. 4.106.2014K).

## REFERENCES

1. V. V. Skopenko, A. Yu. Tsvadze, L. I. Savranskii, and A. D. Garnovskii, *Koordination Chemistry* [in Russian], Akademkniga, Moscow (2007).
2. D. K. Smith and F. Diederich, *Top. Curr. Chem.*, **210**, 183-227 (2000).
3. W.-S. Li and T. Aida, *Chem. Rev.*, **109**, 6047 (2009).
4. B. Donnio, *Inorg. Chim. Acta*, **409**, 53 (2014).
5. V. Balzani, P. Ceroni, A. Juris, et al., *Coord. Chem. Rev.*, **219**, 545 (2001).
6. M. F. Ottaviani, N. D. Ghatlia, S. H. Bossman, et al., *J. Am. Chem. Soc.*, **114**, 8946 (1992).
7. D. Astruc, J.-C. Blais, E. Cloutet, et al., *Top. Curr. Chem.*, **210**, 229-259 (2000).
8. S. H. Hwang, C. D. Shreiner, C. N. Moorefield, and G. R. Newkome, *New J. Chem.*, **31**, 1192 (2007).
9. D. Astruc, E. Boisselier, and C. Ornelas, *Chem. Rev.*, **110**, No. 4, 1857 (2010).
10. C. Gorman, *Adv. Mater.*, **10**, No. 4, 295 (1998).
11. M. A. Halcrow, *Spin-Crossover Materials: Properties and Applications*, John Wiley and Sons, UK (2013).
12. I. Angurell, O. Rossell, and M. Seco, *Inorg. Chim. Acta*, **409**, 2 (2014).
13. M. Seredyuk, A. B. Gaspar, V. Ksenofontov, et al., *Inorg. Chem.*, **47**, No. 22, 10232 (2008).
14. M. Seredyuk, A. B. Gaspar, V. Ksenofontov, et al., *J. Am. Chem. Soc.*, **130**, 1431 (2008).
15. A. V. Pyataev, R. A. Manapov, N. E. Domracheva, et al., *Uch. Zap. Kazan. Univ.*, **154**, No. 3, 26 (2012).
16. H. Luetkens, H.-H. Klauß, R. Benda, et al., *Hyperfine Interact.*, **120/121**, Nos. 1-8, 243 (1999).
17. U. V. Chervonova, M. S. Gruzdev, and A. M. Kolker, *Zh. Obshch. Khim.*, **81**, No. 9, 1515 (2011).
18. U. V. Chervonova, *Dendrimer Azomethine Complexes of Iron(III): Synthesis, Spin States, and Phase Transitions*, Extended Abstract of Cand. Sci. (Chem.) Dissertation, Inst. Khim. Rastvor. Ross. Akad. Nauk, Ivanovo (2012).

19. M. S. Gruzdev, U. V. Chervonova, A. M. Kolker, and A. S. Golubeva, *J. Struct. Chem.*, **53**, No. 5, 845 (2012).
20. Z. Marchenko and M. Bal'tsezhak, *Spectrophotometry Methods in the UV and Visible Ranges in Inorganic Analysis* [in Russian], BINOM, Laboratoriya Znaniy, Moscow (2009).
21. A. W. Baker and A. T. Shulgin, *J. Am. Chem. Soc.*, **81**, 1523 (1959).
22. K. Rathore, R. K. R. Singh, and H. B. Singh, *E-J. Chem.*, **7**, No. S1, S566 (2010).
23. R. Ruiz, J. Sanz, F. Lloret, et. al., *J. Chem. Soc. Dalton Trans.*, 3035 (1993).
24. N. Karaböcek, *Transition Met. Chem.*, **31**, 118 (2006).
25. C. R. Graves, M. L. Merlau, G. A. Morris, et. al., *Inorg. Chem.*, **43**, 2013 (2004).
26. B. Trathnigg, *Prog. Polym. Sci.*, **20**, 615 (1995).
27. I. N. Marov and N. A. Kostromina, *EPR and NMR in the Chemistry of Coordination Compounds* [in Russian], Nauka, Moscow (1979).
28. I.A. Vechkasov, N.A. Kruchinin, A.I. Polyakov, and V.F. Rezinkin, *Instruments and Analysis Methods in the Near Infrared Range* [in Russian], Khimiya, Moscow (1977).
29. E. Pretsch, P. Büllman, and C. Affolter, *Structure Determination of Organic Compounds*, Springer, Berlin (2000).
30. H. Becker, *Organikum: organisch-chemisches Grundpraktikum*, Deutscher Verlag der Wissenschaften (1976).
31. N. Daneshar, A. A. Etezami, A. A. Khandar, and L. A. Saghatforoush, *Polyhedron*, **22**, No. 11, 1437 (2003).
32. L. A. Saghatforoush, A. Aminkhani, and F. Chalabian, *Transition Met. Chem.*, **34**, 899 (2009).
33. M. S. Gruzdev, N. E. Domracheva, U. V. Chervonova, et. al., *J. Coord. Chem.*, **65**, No. 10, 1812 (2012).
34. L. A. Kazitsyna and N. B. Kupletskaia, *Application of UV, IR, and NMR Spectroscopy in Organic Chemistry* [in Russian], Vysshaya Shkola, Moscow (1971).
35. K. Nakanishi, *Infrared Absorption Spectroscopy*, Holden-Day, San Fransisco, Nankodo Company Limited, Tokyo (1962).
36. K. Nakamoto, *Infrared and Raman Spectra of Inorganic and Coordination Compounds*, Wiley (2008).
37. A. Finch, P. N. Gates, K. Radcliffe, F. N. Dickson, and F. F. Bentley, *Chemical Applications of Far Infrared Spectroscopy*, Academic Press (1970).
38. R. J. Cotter, *Time-of-Flight Mass Spectrometry: Instrumentation and Applications in Biological Research*, ACS Professional Reference Books, Washington (1997).
39. V. G. Zaikin, *Mass Spectrometry of Synthetic Polymers* [in Russian], VMSO, Moscow (2009).
40. M. S. Gruzdev, *Effect of the Molecular Structure of Dendrimer Complexes and Nanocomposites – Poly(Propylen Imine) Derivatives – on Their Mesomorphic Properties*, Extended Abstract of Cand. Sci. (Chem.) Dissertation, Ivanovo State University, Ivanovo (2006).
41. V. M. Babaev, *Synthesis and Mass Spectrometry Studies of Isosteviol Diterpenoid Derivatives with Oxygen- and Nitrogen-Containing Fragments*, Cand. Sci. (Chem.) Dissertation, Kazan National Research Technological University, Kazan (2012).
42. A. I. Smirnova and D. W. Bruce, *Zhidk. Krist. Ikh Prakt. Ispol'z.*, **4**, No. 38, 120 (2011).
43. I.-C. Khoo, *Liquid Crystals*, Wiley-Interscience, John Wiley & Sons (2007); I. Dierking, *Textures of Liquid Crystals*, Wiley-VCH Verlag GmbH and Co. KgaA (2003).
44. O. B. Akopova, M. G. Bulavkova, M. S. Gruzdev, and I. Yu. Luk"yanov, *Zhidk. Krist. Ikh Prakt. Ispol'z.*, **2**, No. 32, 46 (2010).
45. Nguyen Huu Tinh, C. Destrade, A.M. Levelut, and J. Malthete, *J. Physique.*, **47**, No. 4, 553 (1986).